*Send Orders for Reprints to reprints@benthamscience.ae*

*The Open Civil Engineering Journal*, 2015, *9*, 489-494


Open Access

# Seismic Damage Study of Asymmetric Continuous Rigid Frame Bridge Based on Nonlinear Time History Analysis

Wu Tong* and Sun Quansheng

*School of Civil Engineering, Northeast Forestry University, Harbin, Heilongjiang, 150040, P.R. China*

**Abstract:** Continuous rigid frame bridge is a common type of bridge in California, where is a seismically active areas. Main structural features of the bridge, including asymmetry, hinge structure, concretion of girder and piers affect the seismic response of the bridge significantly. In order to evaluate the safety of the bridge under earthquake, the nonlinear models of girder, limiting steels in hinge, abutment backfill, abutment bearing, pier are simulated in great detail, and a numerical dynamic overall model, composed of the above components, is made through OpenSees program. On the basis of nonlinear time history analysis with Northridge earthquake load, seismic damage of this kind of bridge is monitored. The research results acquire the accurate damage area of the bridge. Under earthquake, asymmetric continuous rigid frame bridge with curved girder tends to move to the external rim of curve. Asymmetry is detrimental to coinstantaneous vibration of frames, which can cause the large nonlinear damage of limiting steels in hinge. Due to large longitudinal relative seismic response between girder and abutment, the damage of abutment bearing and backfill could be severe. The area on the top and bottom of shorter piers in both sides of bridge is vulnerable because longitudinal steel bars in these areas are liable to yield under repeating shaking of earthquake.

**Keywords:** Seismic damage, asymmetry, continuous rigid frame bridge, OpenSees, time history analysis.

## 1. INTRODUCTION

California, US, is located at San Andreas fault [1], belongs to circum-Pacific seismic belt. Based on this characteristic geological structure, California is a seismically active area. Continuous rigid fame bridges are built commonly in California. Given the difference of river bed altitude, the bridge is often designed to asymmetric type. Continuous bridge is divided into several small continuous rigid fame bridges on account of the design of hinge. Rigid fame indicates girder and piers are consolidated together, which may cause the large seismic response on the top of piers. Seat type are used in the design of abutment widely. With this type of abutment, girder and abutment vibrates independently during earthquake, which may cause the unseating of girder and pounding between girder and abutment back wall. The job of bearings in abutment is to limit the displacement of girder at abutment. If this components damage, relative horizontal displacement between girder and abutment is hard to control.

Some studies focused on the seismic response of seat type abutment, like the studies by Peyman [2] and Stergios [3], and some studies focused on the impact of design parameter to seismic response of hinge, like the studies by DesRoches [4]. Meanwhile, some studies to seismic response of continuous rigid frame bridge were also carried out, like the studies by Shi [5] and Liu [6], however, these studies put emphasis on the overall response of the bridge under earthquake, rather than the detailed nonlinear seismic damage area of the bridge.

*Address correspondence to this author at the School of Civil Engineering, Northeast Forestry University, Harbin, Heilongjiang, 150040, P.R. China; Tel: +86 13936313439;

Considering the importance of bridge safety and the limitation of present studies, a detail model of asymmetric continuous rigid frame bridge was developed through OpenSees. Seismic damage and potential hazard of the bridge was obtained based on nonlinear time history analysis.

## 2. PROJECT PROFILE

Example continuous rigid frame bridge, composed of 8 spans with the length arrangement of 48.8m +64.0m+4×79.3 m+64.0m + 48.8m, was built in the late 1990's, California. The bridge has a curve superstructure with a curvature degree 34°, a radius of 914.4m. All of 7 piers are connected with the girder. Bridge is divided into 3 small frame bridge through designing hinges in two spans. Height of the superstructure section changes from supported point to midpoint of span with parabola. Asymmetric height arrangement of piers, which places longest 5#pier on the right part of bridge, makes the bridge asymmetric. Bridge arrangement was illustrated in Fig. (**1**). The height of every

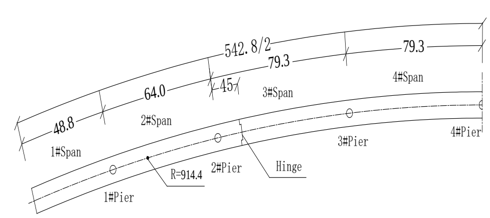


**Fig. (1).** Example bridge arrangement (unit: m).

1874-1495/15 2015 Bentham Open

pier was listed in Table **1**. In occlusive type of hinge, 28 longitudinal limiting steels was given to connect the girders beside hinge, shown in Fig. (**2**). Two two elastomeric bearings was installed in every abutment, shown in Fig. (**3**).

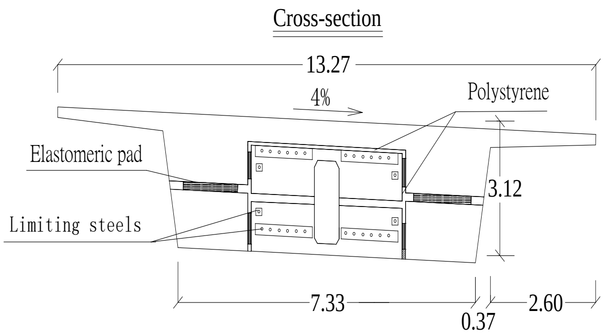


**Fig. (2).** Hinge arrangement(unit: m).

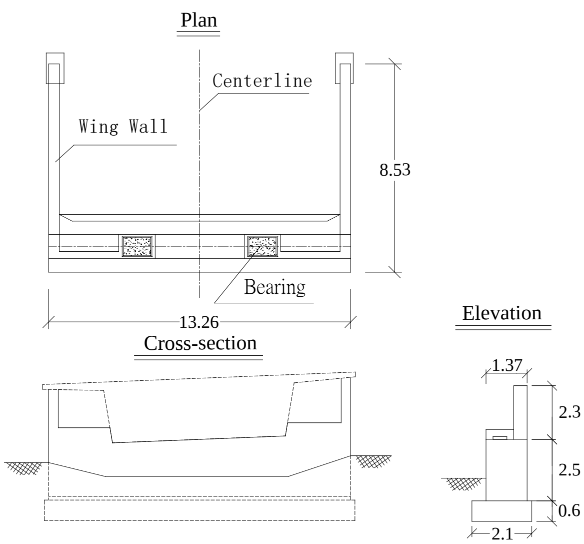


**Fig. (3).** Abutment arrangement (unit: m).

## 3. NUMERICAL MODEL

### 3.1. OpenSees Analysis Platform

Bridge model was implemented by OpenSees(Open System for Earthquake Engineering Simulation), which is a platform aiming at analyzing nonlinear dynamic response and seismic response of engineering structure developed by Peer(Pacific Earthquake Engineering Research Center). In OpenSees, model of example bridge and the global coordinate of model were shown in Fig. (**4**).

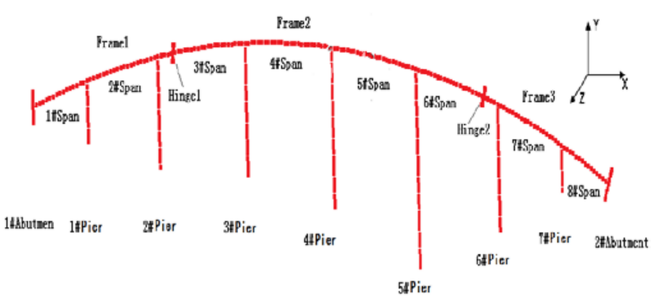


**Fig. (4).** OpenSees numerical model

### 3.2. Material Constitutive Relationship

Chang and Mander's model [7] was used in simulating concrete material. This model, performed by Concrete07 in OpenSees, describes mechanical property for confined concrete and unconfined concrete during complicated loading and unloading process.

Material of steel bar and prestressed tendon was simulated by model from Filippou [8], which considers isotropic strain hardening based on the model from Menegotto and Pinto [9]. Steel02 in OpenSees was used to implement this model.

### 3.3. Simulation of Superstructure and Piers

In earlier research, superstructure was deemed to be elastic during earthquake, so it was simulated by linear element without nonlinear behavior. In this research, in order to obtain accurate damage process of bridge, superstructure was simulated by fiber element having linear and nonlinear behavior, which was the same as that of piers. Displacement-Based Beam-Pier Element in OpenSees, which was given material constitutive relationship, was selected to simulate superstructure element, pier element.

### 3.4. Simulation of Abutment

Seat type was used to design the abutment of example bridge. In each abutment, two bearings are provided to support the superstructure, meanwhile, their shear stiffness limits the longitudinal and transverse displacement of superstructure at abutment. In addition, abutment is restrained by the backfill behind abutment back wall longitudinally. Gap between abutment back wall and superstructure is the sensitive indicator to judge the pounding and unseating damage. Therefore, during dynamic analysis, in order to obtain the damage state of abutment, the nonlinear mechanical relationship of bearings, pounding, spring of soil behind back wall needs to be simulated and monitored.

(1) Abutment Backfill

Shamsabadi and Yan' model [10] was used to simulate the abutment backfill soil in passive response. Fig. (**5**) shows the curve of force and displacement for abutment backfill, where $F_{ult}$ represents the ultimate force corresponding to the ultimate displacement $y_{max}$.

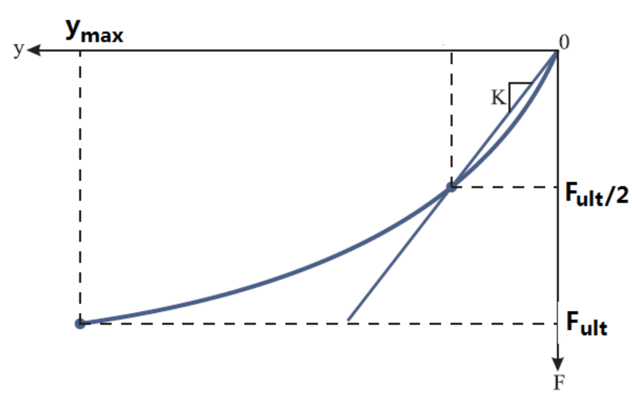


**Fig. (5).** Model of abutment backfill.

**Table 1. Height of piers (unit: m).**

| Pier No. | 1 | 2 | 3 | 4 | 5 | 6 | 7 |
|---|---|---|---|---|---|---|---|
| Height(m) | 12.19 | 23.16 | 28.04 | 34.14 | 42.67 | 26.82 | 8.53 |

(2) Abutment Bearing

Bearing transfers inertial force from superstructure to abutment, as well as dissipate the energy from earthquake through its shear stiffness. When bearing yields in shearing direction, the shear stiffness will decrease to zero. Relationship of displacement and force for bearing was calculated from the study of Scharge [11], shown in Fig. (**6**), where $k_{pad}$ represents initial shear stiffness of bearing, $F_y$ represents yield shear force. Steel01 in OpenSees was used to perform this model.

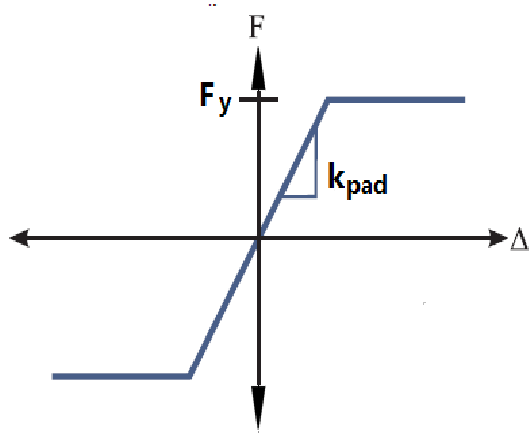


**Fig. (6).** Model of bearing and limiting steel.

(3) Pounding Model

Bilinear model that captures energy dissipation, which was simplified from Hertzdamp model, was used to develop pounding process, shown in Fig. (**7**). Where, $K_{t1}$ is initial stiffness, $K_{t2}$ is yield stiffness, $\delta_y$ is yield displacement, $\delta_m$ is ultimate pounding displacement, $F_m$ is ultimate pounding force, g is the space between elements. The parameters of this mode is from Nielson's proposed value[12].

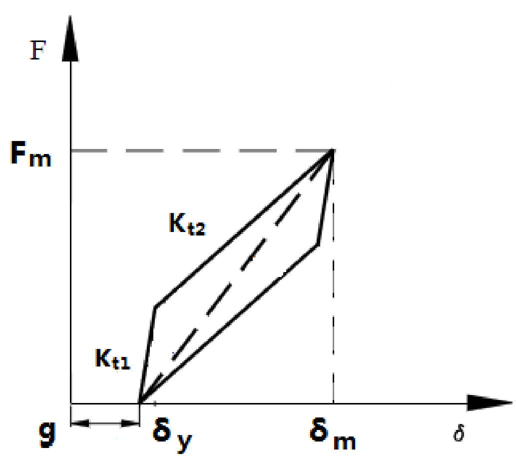


**Fig. (7).** Model of pounding.

### 3.5. Simulation of Hinge

The hinges allow relative longitudinal displacement, but transverse and vertical displacement is restricted by occlusive concrete in hinge [13]. The elastic stiffness and yield strength of longitudinal limiting steels in hinges were calculated. Relationship of force and deformation for longitudinal limiting steels is the same as that for bearing, shown in Fig. (**6**). Steel01 in OpenSees was used to perform this model.

## 4. NONLINEAR TIME HISTORY ANALYSIS

### 4.1. Analysis Theory

After dispersing Multi-DOF system, structural dynamic balance equation is below:

$$M\ddot{u}(t)+C\dot{u}(t)+K\,u(t)=P(t) \tag{1}$$

Where, M represents structural mass matrix, C represents structural damp matrix, K represents structural stiffness matrix, $\ddot{u}(t)$、$\dot{u}(t)$、$u(t)$ represents structural acceleration vector, speed vector and displacement vector respectively. $P(t)$ represents structural load vector.

In theory of time history analysis, duration time T of earthquake load is divided into many time steps $\Delta t$. The relationship between acceleration, speed and displacement, as well as change rule of acceleration, is confirmed in every time step. The dynamic balance equation in the first $\Delta t$ is solved by initial conditions. Solved result serves as the initial conditions for next step. The remaining steps are calculated like last step and so on.

### 4.2. Earthquake Load

Considering the specificity of earthquake in California, Northridge earthquake load was used to perform nonlinear time history analysis. In order to capture the ultimate state of curved bridge, the dynamic load was doubled. Response spectrum and acceleration time history were shown in Figs. (**8**) and (**9**). Acceleration in fault normal, fault parallel, vertical, was loaded, respectively, in longitudinal, transverse and vertical.

### 4.3. Seismic Damage and Response of Bridge

(1) Girder

There was only vertical displacement of girder discussed in former bridge dynamic research. However, due to the curvature, the transverse displacement of girder may be very large under earthquake load. Meanwhile, frame style can also increase seismic response of bridge longitudinally and transversely. Seismic displacement response of girder in three directions were discussed below.

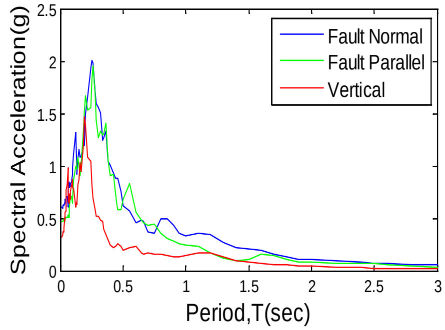


**Fig. (8).** Acceleration response spectrum

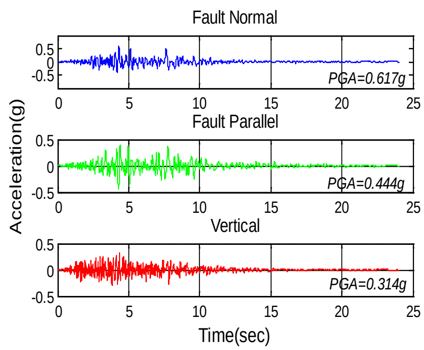


**Fig. (9).** Acceleration time history

Longitudinal displacement time history curves for midpoint of symmetrical spans were illustrated in Fig. (**10**). From them, the moment of extreme value for midpoint of symmetrical spans is roughly same. On account of asymmetry of bridge, there is no obvious overlap for two curves in one figure except the curves for 4# span and 5# span.

It can seen from the last part of curves, the final longitudinal displacement for midpoint of 1#, 2#, 3#, 4#, 5#, 6#span stops in negative direction, whereas the final longitudinal displacement for midpoint of 7#, 8#span stops in positive direction. This phenomenon illustrates the longitudinal displacement of frame1 and frame2 is liable to move to negative X direction and that of frame 3 is liable to move to positive X direction. It implies longitudinal limiting steels in hinge2 may have large nonlinear behavior.

Vertical displacement time history curves for midpoint of symmetrical spans were illustrated in Fig. (**11**). Compared with the longitudinal displacement, vertical displacement is much smaller because of the concretion of girder and piers.

Transverse displacement time history curves for midpoint of symmetrical spans were illustrated in Fig. (**12**). Compared with the longitudinal and the vertical displacement, continuous rigid frame bridge with concretion of girder and piers has larger transverse displacement under earthquake load. The final transverse displacement for midpoint of 2#,3#,4#,5#,6#,7#span stops in negative direction, it implies continuous rigid frame bridge with curved girder tends to move to external rim of curve.

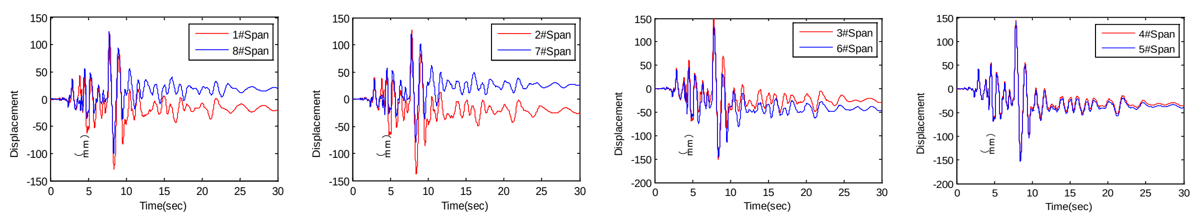


(**a**) 1# and 8# Span (**b**) 2# and 7# Span (**c**) 3# and 6# Span (**d**) 4# and 5# Span

**Fig. (10).** Longitudinal displacement time history for midpoint of spans.

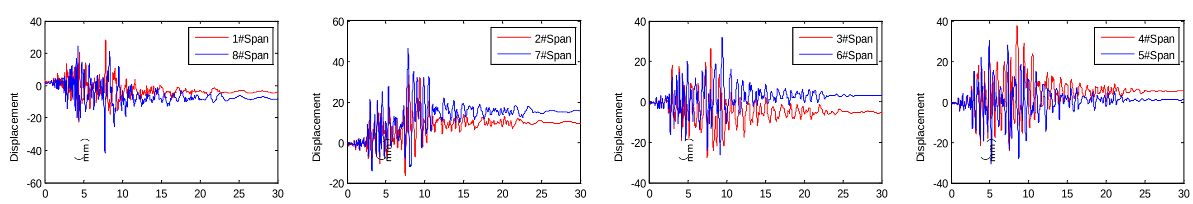


(**a**) 1# and 8# Span (**b**) 2# and 7# Span (**c**) 3# and 6# Span (**d**) 4# and 5# Span

**Fig. (11).** Vertical displacement time history for midpoint of spans.

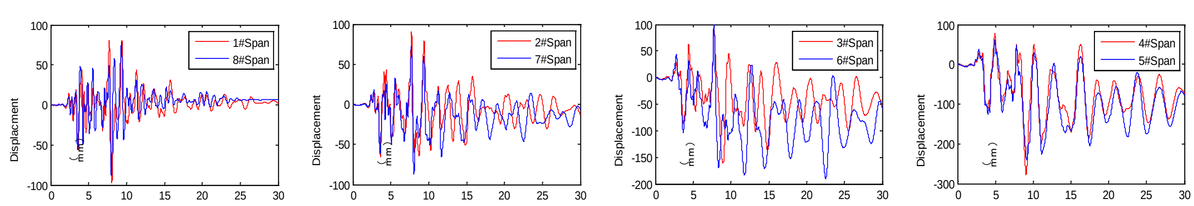


(**a**) 1# and 8# Span (**b**) 2# and 7# Span (**c**) 3# and 6# Span (**d**) 4# and 5# Span

**Fig. (12).** Transverse displacement time history for midpoint of spans.

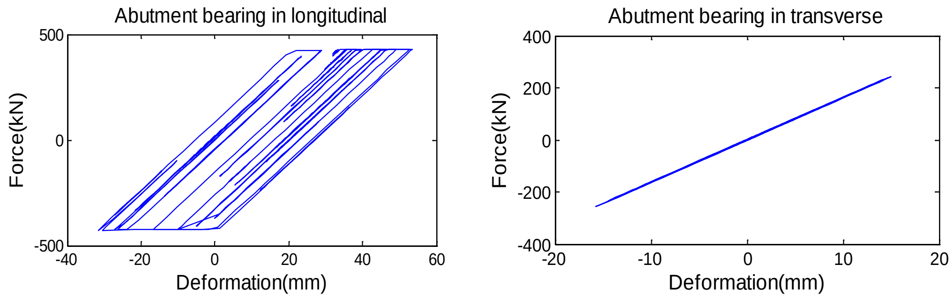


(**a**) Longitudinal (**b**) Transverse

**Fig. (13).** Hysteresis curves for bearing of 0#abutment.

(2) Abutment

Abutment is a crucial function to deliver inertia force from superstructure to soil during earthquake. Large earthquake load can damage some key parts of abutment, like bearing, backfill. Seismic response for key parts of 0#abutment were listed below, and their seismic damage was discussed.

Shear force-deformation hysteresis curves for 0#abutment bearing in longitudinal and transverse were shown in Fig. (**13**). From Fig. (**13**), abutment bearing has yielded in longitudinal but not in transverse. In Fig. (**13, a**), positive maximum seismic deformation of bearing in longitudinal is 53.46mm, and the distance between abutment cap and abutment back wall is 914.4mm, these two data indicates unseating damage of superstructures is hard to happen. In Fig. (**13, b**), bearing in transverse keep elastic.

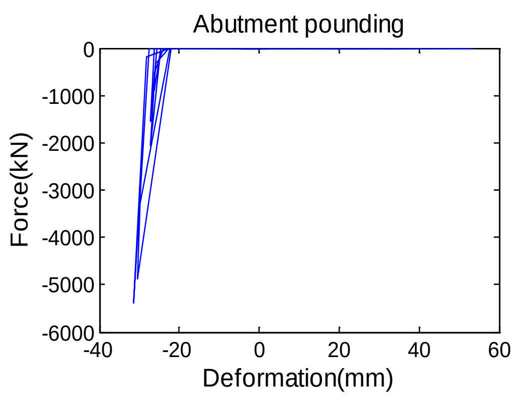


**Fig. (14).** Hysteresis curves for pounding element in 0#abutment.

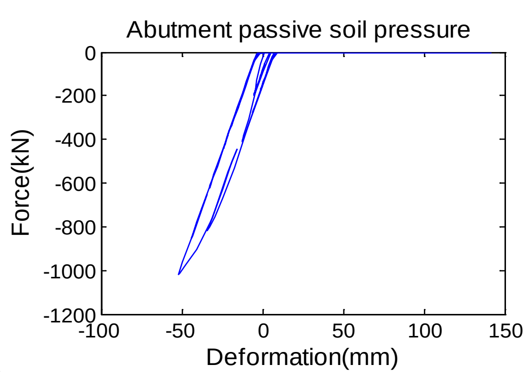


**Fig. (15).** Hysteresis curves of backfill behind 0#abutment.

Pounding force-deformation hysteresis curves for the pounding element between 0#abutment and girder was shown in Fig. (**14**). It indicates pounding happened continually between girder rim and abutment back wall. Maximum deformation of pounding element is the same as negative maximum shear deformation of abutment bearing in longitudinal, which has been shown in Fig.(**13, a**).

Force-deformation hysteresis curve of backfill behind abutment back wall was shown in Fig. (**15**). From Fig. (**15**), backfill, made of clay, has reached to nonlinear state but not reached to yield state. Its maximum compressive deformation is 54.15mm.

(3) Pier

During earthquake, longitudinal steel bars in pier has a main effect to resist repeating earthquake load. With the increasing of earthquake acceleration, the unconfined concrete around external rim of piers begins to crack firstly, then the longitudinal steel bars in every layer begins to yield gradually. Severe damage of steel bars will result in buckling of pier. For ordinary bridge pier, seismic damage always happens on the bottom of it. However, for continuous rigid frame bridge, piers is connected with the superstructure, this kind of design resist the movement on the top of piers and may aggravate damage of this part. Therefore, nonlinear seismic response of piers is extremely important for bridge safety and needs to be monitored.

Maximum strain of longitudinal steel bars for every cross-section along the height of 1#,3#,5#,7#piers was extracted, shown in Fig. (**16**), where $\sigma_y$ is the yield strain of steel bars. From Fig. (**16**), larger response does not only happen on the top of piers, but also the bottom of piers. Piers with shorter height on both sides of bridge have larger response than that with longer height in the middle of bridge. Longitudinal steel bar' strain has passed over the yield strain on the top and bottom of shorter piers, which indicates the possibility of damage in these areas under earthquake load.

## RESEARCH CONCLUSION

The detailed numerical model of asymmetric continuous rigid frame bridge was built using OpenSees. Based on nonlinear time history analysis, the seismic damage of key position of the bridge was studied, and the safety of this kind of bridge was monitored. The main conclusion was listed below:

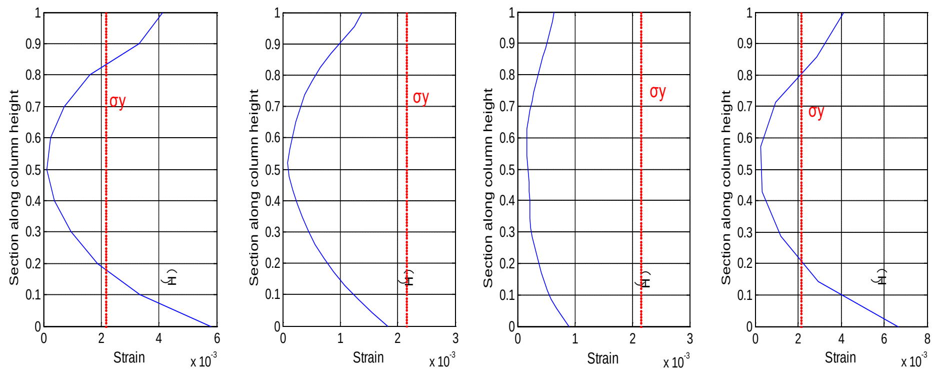


(**a**) 1#Pier (**b**) 3#Pier (**c**) 5#Pier (**d**) 7#Pier

**Fig. (16).** Maximum strain of longitudinal steel bar along pier height**.**

1. For asymmetric continuous rigid frame bridge with curved girder, transverse and longitudinal displacement of girder is larger than vertical displacement. The bridge is liable to move to external rim of curve under earthquake load.
2. Asymmetry can make the frames of bridge vibrate separately. The difference of vibration could lead to the asymmetrical final deformation for every frame, which may give rise to the large nonlinear damage in the longitudinal limiting steels in hinge. If nonlinear damage of limiting steels is too severe, collapse of bridge may happen because of possibility of girder unseating.
3. Large longitudinal seismic response of girder at abutment could cause serious longitudinal nonlinear response of abutment bearing and backfill, as well as the longitudinal pounding between girder and abutment. However, damage of unseating at abutment is hard to happen because of the large distance between abutment cap and abutment back wall.
4. Shorter pier, located at both sides of bridge, is a sensitive component for safety of bridge during earthquake. The seismic damage on the top and bottom of shorter pier is large, and longitudinal steel bars here are liable to yield.

## CONFLICT OF INTEREST

The authors confirm that this article content has no conflict of interest.

## ACKNOWLEDGMENTS

Decleared none.

## REFERENCES

[1] M. Collier, *A Land in Motion: California's San Andreas Fault*, University of California Press: CA, 1999, pp.1-3,

[2] K. Peyman, Z. Farzin, and T. Ertugrul, “Seismic behavior of reinforced concrete bridges with skew-angled seat-type abutments,” *Engineering Structures*, vol. 45, pp. 137-150, 2012.

[3] A. M. Stergios, “Seismic design of bridges with the participation of seat-type abutments,” *Engineering Structures*, vol. 44, pp. 222-233, 2012.

[4] R. DesRoches, and G.L. Fenves, “Design of seismic cable hinge restrainers for bridges,” *Journal of Structural Engineering*, vol. 126, pp. 500–509, 2000.

[5] X.W. Shi, H. P. Liu, Y. J. Zhou, Z. Hu, and Z. Yuan, “Effect of double-thin-wall distance on seismic response of continuous rigid frame bridge,” *Journal of Traffic and Transportation Engineering*, vol. 10, no. 3, pp. 35–40, 2010.

[6] Z.J. Liu, M. Xiong, and Y. Wan, “Seismic reliability analysis of continuous rigid frame bridge using probability density evolution method,”*Journal of Southwest Jiaotong University*, vol. 49, no. 1, pp. 39-44, 2014.

[7] G. Chang, and J. Mander, *Seismic Energy Based Fatigue Damage Analysis of Bridge Piers Part I –Evaluation of Seismic Capacity*, State University of New York at Buffalo: National Center for Earthquake Engineering Research, 1994.

[8] F. C. Filippou, E. Popov, and V. Bertero, *Effects of Bond Deterioration on Hysteretic Behavior of Reinforced Concrete Joints*, Earthquake Engineering Research Center, University of California, Berkeley, 1983.

[9] M. Menegotto, and P.E. Pinto, “Method of analysis for cyclically loaded reinforced concrete plane frames including changes in geometry and non-elastic behavior of elements under combined normal force and bending,” *Proceedings of the IABSE Symposium on Resistance and Ultimate Deformability of Structures Acted on by Well-Defined Repeated Loads*, Lisbon, 1973.

[10] A. Shamsabadi, and L. Yan, “Closed-form force-displacement backbone curves for bridge abutment backfill systems,” In: *Proceedings of the Geotechnical Earthquake Engineering and Soil Dynamics IV Congress*, American Society of Civil Engineers, 2008.

[11] L. Scharge, “Anchoring of bearings by friction, joint sealing and bearing systems for concrete structures,” *World Congress on Joints and Bearings*, Niagara Falls: NY, 1981.

[12] G.B. Nielson, “Analytical *Fragility Curves for Highway Bridges in Moderate Seismic Zones*,” D.S. thesis, Georgia Institute of Technology, Georgia, ON ,USA, 2005.

[13] R. DesRoches, G.L. Fenves, “Evaluation of recorded earthquake response of a curved highway bridge,” *Earthquake Spectra*, vol. 13, no. 3, pp. 363-386, 1997.

Received: April 18, 2015 Revised: May 30, 2015 Accepted: June 05, 2015